

Manuscript Number: CERI-D-16-03294R1

Title: Surface microstructural changes of Spark Plasma Sintered zirconia after grinding and annealing

Article Type: Full length article

Keywords: zirconia; SPS; grinding; annealing; grain size; low temperature degradation

Corresponding Author: Ms. latifa melk, Ph.D.

Corresponding Author's Institution: Universitat Politècnica de Catalunya (UPC)

First Author: latifa melk, Ph.D.

Order of Authors: latifa melk, Ph.D.; Johanne Mouzon, Associate Professor; Miquel Turon-Vinas, PhD; Farid Akhtar, Associate Professor; Marta-Lena Antti, Professor; Marc Anglada, Professor

Abstract: Spark plasma sintered zirconia (3Y-TZP) specimens have been produced of 140 nm 372 nm and 753 nm grain sizes by sintering at 1250 °C, 1450 °C and 1600°C, respectively. The sintered zirconia specimens were grinded using a diamond grinding disc with an average diamond particle size of about 60 µm, under a pressure of 0.9 MPa. The influence of grinding and annealing on the grain size has been analysed. It was shown that thermal etching after a ruff grinding of specimens at 1100 °C for one hour induced an irregular surface layer of about a few hundred nanometres in thickness of recrystallized nano-grains, independently of the initial grain size. However, if the ground specimens were exposed to higher temperature, e.g. annealing at 1575 °C for one hour, the nano-grain layer was not observed. The resulted grain size was similar to that achieved by the same heat treatments on carefully polished specimens. Therefore, by appropriate grinding and thermal etching treatments, nanograined surface layer can be obtained which increases the resistance to low temperature degradation.

Dear Dr. Pietro Vincenzini  
General Editor  
Ceramics International

Many thanks for accepting the manuscript ref "CERI-D-16-03294" for publication in Ceramics International. We are enclosing the manuscript with the changes suggested by reviewers.

Yours sincerely,  
Latifa Melk

Dear Editor

In this manuscript, we studied the effect of grinding on 3Y-TZP sintered using Spark Plasma Sintering (SPS) at three different SPS temperatures 1250 °C, 1450 °C and 1575 °C which induces different grain sizes 140 nm, 372 nm and 753 nm respectively. The surface microstructural changes on the grain size after grinding and annealing were investigated.

To the best of our knowledge, this is the first time, the microstructural changes after grinding zirconia sintered by SPS is studied. The current study showed that a thermal etching at 1100 °C after grinding the samples induces a surface layer of recrystallized nanograins in the range of few hundred nanometers. However, the annealing of ground specimens at high temperature results in high grain sizes similar to that achieved by the same heat treatment on polished specimens.

We hope you find this manuscript interesting and worth publishing

Best regards

Latifa Melk

1                   Surface microstructural changes of Spark Plasma Sintered zirconia  
2  
3                                   after grinding and annealing  
4  
5  
6  
7

8                   |           Latifa Melk<sup>a, b, c, d</sup>, Johanne Mouzon<sup>e</sup>, Miquel Turon<sup>a, b</sup>, Farid Akhtar<sup>c</sup>,  
9  
10                                   Marta-Lena Antti<sup>c</sup>, Marc Anglada<sup>a, b</sup>  
11  
12  
13

14                   <sup>a</sup> CIEFMA-Department of Materials Science and Metallurgical Engineering,  
15                   ETSEIB, Universitat Politècnica de Catalunya, 08028 Barcelona, Spain  
16  
17

18                   <sup>b</sup> CRnE, Campus Diagonal Sud, Edifici C', Universitat Politècnica de Catalunya,  
19                   08028 Barcelona, Spain  
20  
21

22                   <sup>c</sup> Department of Engineering Sciences and Mathematics, Luleå University of  
23                   Technology, 97187 Luleå, Sweden  
24  
25

26                   |           <sup>e</sup> Department of Civil, Environmental and Natural Resources Engineering, Luleå  
27                   University of Technology, 97187 Luleå, Sweden  
28  
29  
30  
31  
32  
33  
34  
35  
36  
37  
38  
39  
40  
41  
42  
43  
44  
45  
46  
47  
48  
49  
50  
51

52                   |           <sup>d</sup> Corresponding author at: Department of Materials Science and  
53                   Engineering/ETSEIB  
54                   Diagonal 647. 08028-Barcelona  
55                   Tel. +34 934016701  
56                   Fax. +34 934016706  
57                   E-mail: melk.latifa@gmail.com  
58  
59  
60  
61  
62  
63  
64  
65

## Abstract

Spark plasma sintered zirconia (3Y-TZP) specimens have been produced of 140 nm, 372 nm and 753 nm grain sizes by sintering at 1250 °C, 1450 °C and 1600°C, respectively. The sintered zirconia specimens were grinded using a diamond grinding disc with an average diamond particle size of about 60 µm, under a pressure of 0.9 MPa. The influence of grinding and annealing on the grain size has been analysed. It was shown that thermal etching after a rough grinding of specimens at 1100 °C for one hour induced an irregular surface layer of about a few hundred nanometres in thickness of recrystallized nano-grains, independently of the initial grain size. However, if the ground specimens were exposed to higher temperature, e.g. annealing at 1575 °C for one hour, the nano-grain layer was not observed. The resulted grain size was similar to that achieved by the same heat treatments on carefully polished specimens. Therefore, by appropriate grinding and thermal etching treatments, nanograined surface layer can be obtained which increases the resistance to low temperature degradation.

**Keywords:** zirconia; SPS; grinding; annealing; grain size; low temperature degradation

# 1 Introduction

Yttria stabilised tetragonal polycrystalline zirconia (3Y-TZP) has a wide range of applications, especially in the medical sector, because of its biocompatibility and very good mechanical properties, such as strength and toughness. The local and constrained phase transformation from tetragonal (*t*) to monoclinic (*m*) structure generates compressive stresses at the crack tip which enhances toughness. However, 3Y-TZP suffers from surface spontaneous *t-m* transformation in humid atmosphere, often referred to as hydrothermal degradation, aging or low temperature degradation (LTD), which is accompanied by formation of near surface microcracks and loss of surface mechanical properties [1-4].

During the processes of final shaping and surface finishing, 3Y-TZP may be subjected to different machining processes (cutting, polishing, grinding, and milling). The damage induced by machining affects structural integrity and reliability of the material. Therefore, machining zirconia is considered as a critical step in the manufacturing of long lasting and strong 3Y-TZP components.

Previous investigations have shown that grinding influences the surface integrity and the flexural strength of 3Y-TZP materials [5]. Therefore, most of the studies on ground zirconia have focussed on characterizing surface microstructural changes that may affect the chemical and mechanical behaviour. The main changes frequently observed in the X-ray diffraction (XRD) spectrum are the following: (1) *t-m* phase transformation; (2) asymmetrical broadening of the (1 1 1) tetragonal peak at  $\approx 30^\circ$  ( $2\theta$ ); (3) intensity reversal of the tetragonal doublet at  $34.64^\circ$  and  $35.22^\circ$  ( $2\theta$ ) corresponding to the (0 0 2) and (2 0 0) planes [6-10]. On the other hand, a TEM investigation of the ground surface by Munoz et al. [11] reported the existence of three different regions from the ground surface towards the bulk : (1) a recrystallized zone, exactly at the surface, where the grains have a diameter in the range 10-20 nm; (2) a plastically deformed zone; (3) a *t-m* transformed zone, which is mainly responsible for the formation of compressive residual stresses that usually increase the flexure strength and the apparent fracture toughness of ground specimens [11].

The near surface monoclinic phase formed during machining operations can be reversed to tetragonal by annealing. The operation of grinding and the time and temperature of annealing have an influence on the resistance to LTD, which can be inhibited or delayed [12]. The evolution of the resistance to LTD of specimens

1 of initially 330 nm grain size subjected to grinding and annealing at 1200 °C for  
2 different times (1 min, 10 min and 1h) was analysed by Muñoz et al. [13]. The  
3 results showed that LTD of ground 3Y-TZP was suppressed due to the formation of  
4 a recrystallized nano-grain layer on the surface. Moreover, the resistance to LTD  
5 was decreasing during long time annealing at 1200 °C after that grain size reached  
6  
7 grew beyond the initial surface grain size of 330 nm. The effect of different high  
8 annealing temperatures in the range 1200°C - 1600°C on the surface  
9 microstructure of ground zirconia was recently studied by Roa et al. [14]; they also  
10 found the recrystallized surface nano-grain layer after annealing at 1200 °C by  
11 milling a small cross section of the near surface region by FIB/SEM, while at 1600  
12 °C the near surface microstructure was composed of larger grain sizes than the  
13 grain size of the bulk material.  
14  
15  
16  
17  
18  
19

20 To the best of our knowledge, previous studies of the effect of grinding has been  
21 carried out only on 3Y-TZP with grain size around 330 nm sintered using  
22 conventional methods. However, the aim of this work is to study the of surface  
23 microstructural changes after grinding and annealing on grains in the range of  
24 140-370 nm produced by Spark Plasma Sintered (SPS) at 1250 °C and 1600 °C,  
25 respectively.  
26  
27  
28  
29  
30

## 31 **2 Experimental**

### 32 *2.1 Material processing*

33  
34  
35  
36  
37  
38 Zirconia powder stabilized with 3 mol % of yttria (TZ-3YSB-E, Tosoh, Tokyo,  
39 Japan) with a crystalline size of 36 nm was sintered using spark plasma sintering  
40 (SPS) at 1250 °C, 1450 °C and 1600 °C for 5 minutes. The pressure maintained  
41 during the sintering cycle was 55 MPa and the heating rate was 100 °C/min.  
42  
43

44  
45 The final samples were ceramic discs (50 mm x 3 mm). The average grain size was  
46 determined using the line intercept method on SEM images and the density was  
47 measured by the Archimedes method.  
48  
49  
50

51 The samples were ground using a new diamond grinding disc (MD-Piano 220  
52 Struers) with an average particle size of about 60 µm, under a pressure of 0.9 MPa  
53 with a constant grinding speed of 3.6 m/s in one direction and water cooling.  
54 The selection of this grinding condition was based on a previous work of Juy et al.  
55 [15], who found that these particular parameters produce an increase in  
56 mechanical properties. The samples were then thermally etched at 1100 °C for 1  
57  
58  
59  
60  
61

1 hour in standard furnace in air in order to observe grain size in the scanning  
2 electron microscope (SEM).

3  
4 The samples studied will be referred to as SPS 1250, SPS 1450 and SPS 1600  
5 according to the temperature used for sintering at 1250 °C, 1450 °C and 1600  
6 °C, respectively. The samples were divided into two batches. The first batch  
7 corresponds to the as-ground samples which are referred in the current study as  
8 GRD (as ground). In order to reveal the grain size of the GRD samples, they were  
9 maintained at 1100 °C for 1 hour for thermal etching, 1200 °C for annealing,  
10 and at 1575 °C for high temperature annealing. The second batch consists of  
11 specimens that were polished starting with 9 µm diamond down to 1 µm and  
12 finally polished with colloidal silica. The polished samples were subjected to the  
13 same heat treatment temperatures, and are herein referred to as POL (as  
14 polished). In fact, each heat treatment on ground and polished specimens was  
15 carried out on the very same sample by polishing one face of the disc and grinding  
16 the other face in order to ensure that both faces were exactly subjected to the  
17 same temperature during annealing.  
18  
19  
20  
21  
22  
23  
24  
25  
26  
27  
28

## 29 *2.2 Mechanical testing*

30  
31  
32 Hardness was measured by Vickers indentation with a load of 98.1 N. The cracks  
33 emanating from the vertex of the residual impressions were used to measure  
34 indentation fracture toughness using Niihara equation [16] taking into account  
35 the observed Palmqvist configuration of the indentation cracks. Anstis et al. [17]  
36 equation was also applied for comparative purposes. However, as extensively  
37 reported in the literature [18], indentation fracture toughness does not really  
38 represent the "true" fracture toughness ( $K_{Ic}$ ) of the material. Therefore, the  
39 fracture toughness measurements in the present work have been used only as an  
40 indication of *tm* transformability under localised sharp contact of compressive  
41 loads.  
42  
43  
44  
45  
46  
47  
48  
49

## 50 *2.3 Surface Analysis*

51  
52  
53 The crystallographic phases were identified by X-ray diffraction (XRD) with Bragg-  
54 Brentano symmetric-geometry, using PANalytical Empyrean equipment with  
55 PIXcel-3D detector and Cu-K $\alpha$  (45kV and 40mA) radiation. The XRD spectra  
56 were obtained in a scan range of  $20^\circ \leq 2\theta \leq 100^\circ$ , using a step size of  $0.013^\circ$  and an  
57  
58  
59  
60  
61  
62  
63  
64  
65



anti-scatter slit of 1°. The monoclinic phase content was calculated by the equation proposed by Toraya et al. [19].

$$V_m = \frac{1.311 \times (I_m^{(\bar{1}11)} + I_m^{(111)})}{1.311 \times (I_m^{(\bar{1}11)} + I_m^{(111)}) + I_t^{(111)}}$$

Surface damage analysis of all the specimens was performed by extreme high resolution scanning electron microscopy (XHR-SEM) (Magellan 400, FEI Company) at an acceleration voltage of 3 kV. Microstructural changes below the surface induced during the grinding process were investigated by preparing thin cross-sections using focused ion beam (FIB). Cross sectioning observations were conducted using a dual beam workstation (Zeiss Neon 40). A thin platinum layer was deposited on the sample prior to FIB with the aim of reducing ion-beam damage. A Ga<sup>+</sup> ion source was used to mill the surface at a voltage of 30kV. Final polishing of the cross-section was performed at a current of 500 pA.

### 3 Results and discussion

**Table 1** shows clearly that the use of SPS results in dense zirconia samples of about 99% of theoretical density. SPS is a highly efficient technique for the densification of zirconia ceramics compared with conventional sintering such as Hot Pressing (HP) for example. Self-heating from spark discharge between the particles could be the reason behind the low temperature and short time for sintering. It has been found that during SPS the residual gases in the powder will be efficiently removed as long as the system is open. As the pressure will not be applied until the isothermal temperature is reached, CO<sub>2</sub>(g) and H<sub>2</sub>O(g) can then escape before the densification starts [20].

Furthermore, by increasing the SPS temperature, the grain size increases from 140 nm to 750 nm for SPS 1250 and SPS 1600, respectively, see **Table 2** and **Fig. 1**. It has been reported that the presence of an electric field could enhance the grain growth in yttria-stabilized cubic zirconia by increasing the grain boundary mobility [21]. Moreover, a dependency was shown between grain size and the heating-rate which promoted grain growth by increasing the defect concentration [22].

**Fig. 2** shows the XRD spectra of GRD in all SPS zirconia samples. It can be observed the presence of a broadening of the tetragonal peaks and that the tetragonal peak at 2θ≈30° that corresponds to (111)<sub>t</sub> has a peak shoulder that

1 may correspond to either the rhombohedral phase or to distorted tetragonal  
2 phase as was reported in [14]. The presence of monoclinic phase at  $2\theta \approx 28, 16^\circ$   
3 was also observed. It has been found that the monoclinic phase detected in GRD  
4 is 13 %, 14 % and 12 % for SPS 1250, SPS 1450 and SPS 1600 respectively, see  
5 **Fig. 3**.  
6  
7

8  
9 After annealing at 1200 °C and 1575 °C, the peak shoulder disappears and no  
10 monoclinic phase is detected due to the *m-t* transformation that actually starts at  
11 lower temperatures [23]. It could also be observed that the intensity of (002) and  
12 (200) tetragonal peaks at  $2\theta = 34, 64^\circ$  and  $35, 22^\circ$  is reversed compared to the POL.  
13 In POL, the intensity ratio of  $I_t^{(002)}/I_t^{(200)}$  is equal to 0.45 while in GRD  
14 annealed at 1575 °C,  $I_t^{(002)}/I_t^{(200)}$  the ratio is equal to 1.63. This is attributed to  
15 the texture due stress induced reorientation from ferroelastic domain switching  
16 [7].  
17  
18  
19  
20  
21  
22

23 Indentation fracture toughness is similar to that for conventionally sintered 3Y-  
24 TZP with similar grain size, independently of the indentation equation used for  
25 calculating the fracture toughness. On the other hand, there is a small decrease in  
26 hardness with grain size which may be related to a higher transformability as the  
27 grain size increases, see **Table 2**.  
28  
29  
30  
31

32 The specimens GRD with subsequent thermal etching at 1100 °C for 1 hour  
33 show a nanometric grain size on the surface as can be seen on the images of left  
34 column of **Fig. 3**. The larger grain size observed in GRD was always much smaller  
35 than the average grain size in POL. After thermal etching at 1100 °C, the grain  
36 size in the GRD was reduced by a factor of 2 compared to the POL in SPS 1250  
37 and by a factor of 10 in SPS 1575. However, if GRD specimens are annealed at  
38 1200 °C or 1545 °C, the surface grain size increases fast and it reaches  
39 dimensions roughly similar to as POL specimens subjected to the same high  
40 temperature treatment. This can be appreciated by comparing GRD and POL  
41 specimens under the same heat treatment (see **Fig. 3**).  
42  
43  
44  
45  
46  
47  
48  
49

50 The analysis of sections perpendicular to the surface obtained by FIB (**Fig. 4**)  
51 shows that there is a very thin layer of surface damage on GRD specimens after  
52 grinding. The layer extends to depths of only a few hundred nanometers. The  
53 depth is not uniform and it changes from one place to another. It is deeper close  
54 to places where the material is piling up at the side of the grinding scratches. The  
55 same observation was carried out after annealing and they are shown in **Fig. 5**.  
56  
57  
58  
59  
60  
61  
62  
63  
64  
65

1 **Fig. 5** shows the presence of the nano-grain layer with a depth corresponding to  
2 the same depth of the nano-grain layer seen in the ground specimens before  
3 annealing.  
4

5 The existence of this surface nano-grain size layer on thermal etched GRD  
6 specimens can also be detected on the fracture surface of specimens as shown in  
7 **Fig. 6** where the fracture surface of POL and GRD are compared. The presence of  
8 nano-grain layer in the etched GRD specimens can be clearly observed. This nano-  
9 grain layer is formed by recrystallization of a very thin highly deformed surface  
10 layer produced during grinding. Since the usual procedure to observe the grain  
11 size is by means of grinding with decreasing diamond particle size and careful  
12 polishing, the damage layer is finally removed so that no recrystallization is  
13 detected during standard specimen preparation and thermal etching for grain size  
14 determination.  
15  
16  
17  
18  
19  
20  
21

22  
23 In one of the earliest investigations on this topic [12], it was shown that this  
24 recrystallized nanometric layer can be useful for preventing hydrothermal  
25 degradation because the resistance to LTD increases as the zirconia grain size  
26 decreases. The requirement of a smooth polished surface for many applications  
27 makes this procedure feasible when a specular smooth surface finish is not  
28 required. It may be of interest when a rough surface is beneficial as for example  
29 for implants since roughness favours osseointegration [24].  
30  
31  
32  
33  
34

35 Regarding the influence of the surface damage induced by grinding on the  
36 strength, it was shown that it does not affect the strength of ground specimens.  
37 On the contrary, grinding induces the formation of a compressive surface layer  
38 which results in an increase of the strength [25,26]. However, after thermal  
39 etching and recrystallization, the compressive forces disappear as monoclinic  
40 phase is transformed back to tetragonal and then the strength may slightly  
41 decrease depending on the damage induced by grinding [11].  
42  
43  
44  
45  
46  
47

48 It is still unknown how much minimum plastic deformation by grinding is  
49 needed in order to form nanocrystals during etching. It will be interesting to find  
50 out which are the weakest grinding conditions for which recrystallization still  
51 takes place during thermal etching. **Fig. 7** shows a shallow scratch left on a  
52 polished surface where recrystallization still takes place in and around the scratch.  
53 This shows that the recrystallization could still remain after polishing if a deep  
54  
55  
56  
57  
58  
59  
60  
61  
62  
63  
64  
65

1  
2 scratch is not fully removed by subsequent operations of grinding with smaller  
3 particle size followed by polishing.

#### 4 **Conclusions**

5  
6  
7 Spark plasma sintered 3Y-TZP specimens have been produced with different grain  
8 sizes of 140 nm, 372 nm and 753 nm by sintering at 1250 °C, 1450 °C and 1600  
9 °C. The influence of grinding and annealing has been analysed. Two main  
10 conclusions can be derived from the present work: a) the effect of the grinding  
11 conditions used in this study induces a few hundred nanometer surface layer  
12 which recrystallizes during thermal etching at 1100 °C. The surface layer contains  
13 recrystallized nano-grains with a grain size smaller and practically independent of  
14 the initial grain size depending on the SPS temperature. This behaviour is similar  
15 to that of conventionally sintered zirconia specimens; b) if the ground layer is  
16 exposed to higher annealing temperatures, the nano-grain layer disappears and  
17 the surface grains grow to a size which is similar to that achieved in polished  
18 specimens by heat treatment to the same temperature. The nano-grain layer  
19 formation could ~~inhibit~~inhibit the low temperature degradation.  
20  
21  
22  
23  
24  
25  
26  
27  
28  
29  
30

#### 31 **Acknowledgements**

32  
33 The authors gratefully acknowledge the financial support given by the “Ministerio  
34 de Ciencia e Innovación”, Spain through research grant MAT2014-60720-R. The  
35 authors acknowledge the EU for financial support through the e-Create-Network  
36 of the Rise program. L. Melk acknowledges the fellowship award received from  
37 the European Joint Doctoral Programme in Materials Science and Engineering  
38 (DocMASE) of the European Union. Finally, all authors thank Dr. Trifon  
39 Trifonov and Dr. Joan Josep Roa from UPC for their assistance in the FIB/SEM  
40 equipment.  
41  
42  
43  
44  
45  
46  
47  
48  
49  
50  
51  
52  
53  
54  
55  
56  
57  
58  
59  
60  
61  
62  
63  
64  
65

1  
2  
3  
4  
5  
6  
7  
8  
9  
10  
11  
12  
13  
14  
15  
16  
17  
18  
19  
20  
21  
22  
23  
24  
25  
26  
27  
28  
29  
30  
31  
32  
33  
34  
35  
36  
37  
38  
39  
40  
41  
42  
43  
44  
45  
46  
47  
48  
49  
50  
51  
52  
53  
54  
55  
56  
57  
58  
59  
60  
61  
62  
63  
64  
65

## References

- [1] K. Kobayashi, H. Kuwajima, T. Masaki, Phase change and mechanical properties of  $\text{ZrO}_2\text{-Y}_2\text{O}_3$  solid electrolyte after ageing, *Solid State Ionics*. 3 (1981)489-493.
- [2] M. Yoshimura, T. Noma, K. Kawabata, S. Somiya, Role of  $\text{H}_2\text{O}$  on the degradation process of Y-TZP, *J. Mat. Sci Lett*. 6 (2000) 465-467.
- [3] S. Lawson, Environmental Degradation of Zirconia Ceramics, *J. Eur. Ceram. Sci*. 15 (1995) 485-502.
- [4] J. Chevalier, L. Gremillard, A. V. Virkar, D.R. Clarke, The Tetragonal-Monoclinic Transformation in Zirconia: Lessons Learned and Future Trends, *J. Am. Ceram. Soc*. 92 (2009) 1901-1920.
- [5] T. Kosmač, Č. Oblak, P. Jevnikar, N. Funduk, L. Marion, Strength and reliability of surface treated Y-TZP dental ceramics, *J. Biomed. Mater. Res*. 53 (2000) 304-313.
- [6] H. Hasegawa, Rhombohedral phase produced in abraded surfaces of partially stabilized zirconia (PSZ), *J. Mater. Sci. Lett*. 2 (1983) 91-93.
- [7] A. V. Virkar, R.L.K. Matsumoto, Ferroelastic Domain Switching as a Toughening Mechanism in Tetragonal Zirconia, *J. Am. Ceram. Soc*. 69 (1986) C-224-C-226.
- [8] J. Kitano, Y. Mori, A. Ishitani, T. Masaki, A Study of Rhombohedral Phase in  $\text{Y}_2\text{O}_3$ -Partially Stabilized Zirconia, *MRS Proc*. 78 (1986) 17.
- [9] N. Mitra, K. Vijayan, B. Bai, S.K. Biswas, Phase Transformation Introduced

- 1  
2  
3  
4  
5  
6  
7  
8  
9  
10  
11  
12  
13  
14  
15  
16  
17  
18  
19  
20  
21  
22  
23  
24  
25  
26  
27  
28  
29  
30  
31  
32  
33  
34  
35  
36  
37  
38  
39  
40  
41  
42  
43  
44  
45  
46  
47  
48  
49  
50  
51  
52  
53  
54  
55  
56  
57  
58  
59  
60  
61  
62  
63  
64  
65
- by Mechanical and Chemical Surface Preparations of Tetragonal Zirconia Polycrystals, *J. Am. Ceram. Soc.* 76 (1993) 533–535.
- [10] D.P. Burke, W.M. Rainforth, Intermediate rhombohedral ( $r\text{-ZrO}_2$ ) phase formation at the surface of sintered Y-TZP's, *J. Mater. Sci. Lett.* 16 (1997) 883–885.
- [11] J.A. Munz-Tabares, E. Jiménez-Piqué, J. Reyes-Gasga, M. Anglada, Microstructural changes in ground 3Y-TZP and their effect on mechanical properties, *Acta Mater.* 59 (2011) 6670–6683.
- [12] P.J. Whalen, F. Reidinger, R.F. Antrim, Prevention of low-temperature surface transformation by surface recrystallization in yttria-doped tetragonal zirconia, *J. Am. Ceram. Soc.* 72 (1989) 319–321.
- [13] J.A. Muñoz-Tabares, M. Anglada, Hydrothermal degradation of ground 3Y-TZP, *J. Eur. Ceram. Soc.* 32 (2012) 325–333.
- [14] J.J. Roa, M. Turon-Vinas, M. Anglada, Surface grain size and texture after annealing ground zirconia, *J. Eur. Ceram. Soc.* 36 (2016) 1519–1525.
- [15] A. Juy, M. Anglada, Surface phase transformation during grinding of Y-TZP, *J. Am. Ceram. Soc.* 90 (2007) 2618–2621.
- [16] K. Niihara, A fracture mechanics analysis of indentation-induced Palmqvist crack in ceramics, *J. Mater. Sci. Lett.* 2 (1983) 221–223.
- [17] G.R. Anstis, P. Chantikul, B.R. Lawn, D.B. Marshal, A critical evaluation of indentation techniques for measuring fracture toughness: I Direct crack measurements, *J. Am. Ceram. Soc.* 46 (1981) 533–538.
- [18] G.D. Quinn, R.C. Bradt, On the Vickers Indentation Fracture Toughness Test, *J. Am. Ceram. Soc.* 90 (2007) 673–680.
- [19] H. Toraya, M. Yoshimura, S. Somiya, Calibration Curve for Quantitative Analysis of the Monoclinic-Tetragonal  $\text{ZrO}_2$  System by X-Ray Diffraction, *Commun. Am. Ceram. Soc.* (1984) 119–121.
- [20] P. Dahl, I. Kaus, Z. Zhao, M. Johnsson, M. Nygren, K. Wiik, et al., Densification and properties of zirconia prepared by three different sintering techniques, *Ceram. Int.* 33 (2007) 1603–1610.
- [21] S.W. Kim, S.G. Kim, J. Il Jung, S.J.L. Kang, I.W. Chen, Enhanced grain boundary mobility in yttria-stabilized cubic zirconia under an electric current, *J. Am. Ceram. Soc.* 94 (2011) 4231–4238.
- [22] B.N. Kim, K. Hiraga, K. Morita, H. Yoshida, Effects of heating rate on microstructure and transparency of spark-plasma-sintered alumina, *J. Eur. Ceram. Soc.* 29 (2009) 323–327.

- 1  
2  
3  
4  
5  
6  
7  
8  
9  
10  
11  
12  
13  
14  
15  
16  
17  
18  
19  
20  
21  
22  
23  
24  
25  
26  
27  
28  
29  
30  
31  
32  
33  
34  
35  
36  
37  
38  
39  
40  
41  
42  
43  
44  
45  
46  
47  
48  
49  
50  
51  
52  
53  
54  
55  
56  
57  
58  
59  
60  
61  
62  
63  
64  
65
- [23] O. Fabrichnaya, F. Aldinger, Assessment of thermodynamic parameters in the system  $ZrO_2$ - $Y_2O_3$ - $Al_2O_3$ , *Zeitschrift Für Met.* 95 (2004) 27-39.
  - [24] Q. Flamant, F. García Marro, J.J. Roa Rovira, M. Anglada, Hydrofluoric acid etching of dental zirconia. Part 1: etching mechanism and surface characterization, *J. Eur. Ceram. Soc.* 36 (2016) 121-134.
  - [25] A. Juy, L. Llanes, M. Anglada, Strength of Yttria-Stabilised Zirconia with Near-Surface Grinding Residual Stresses, ECF14, Cracow 2002. (2013).
  - [26] T. K. Gupta, Strengthening by Surface Damage in Metastable Tetragonal Zirconia, *J. Am. Ceram. Sci.* 63 (1980) 117.

**Table 1.** Density and grain size of the SPS zirconia specimens before and after annealing.

**Table 2.** Vickers hardness and indentation fracture toughness of the SPS zirconia samples.



**Table 1**

Specimen	Density (g.cm <sup>-3</sup> )	Temperature/Grain size					
		1100°C POL (nm)	1100°C GRD (nm)	1200°C POL (nm)	1200°C GRD (nm)	1575°C POL (nm)	1575°C GRD (nm)
SPS1250	6.00 ±0.03	140±10	59±7	144±16	105±9	611±93	602±153
SPS1450	5.99± 0.09	372±50	66±15	386±29	149±22	699 ±79	896±167
SPS1600	6.05± 0.04	753±60	67±11	658±76	±	856±57	708±97

**Table 2**

Specimen	Vickers hardness (HV10) (GPa)	Indentation $K_{IC}$ (Niihara) (MPa·m <sup>1/2</sup> )	Indentation $K_{IC}$ (Anstis) (MPa·m <sup>1/2</sup> )
SPS 1250	14.7±0.2	5.2±0.1	3.9±0.2
SPS 1450	13.8±0.1	5.1±0.1	3.8±0.1
SPS 1600	13.6±0.2	5.2±0.1	4.0±0.1

**Fig. 1** SEM images showing the microstructure of POL after thermal etching at 1100 °C for 1h: **a)** SPS 1250 **b)** SPS1450 and **c)** SPS1600.

**Fig. 2** XRD spectra of SPS zirconia POL, GRD, GRD+annealed at 1200 °C and GRD+annealed at 1575 °C.

**Fig. 3** Grain size of GRD SPS specimens after thermal etching for 1 hour at the temperatures indicated on the top row.

**Fig. 4** Microstructure of GRD below the surface **a)** SPS 1250; **b)** SPS1450 and **c)** SPS 1600 after grinding and before thermal etching.

**Fig. 5** Microstructure of GRD after thermal etching **a)** SPS 1250 top left **b)** SPS1450 top right **c)** SPS 1600 bottom after grinding and thermal etching.

**Fig. 6** Fracture surfaces of POL (top) and GRD (bottom) SPS1250. General views on the left and high magnification details of the surfaces on the right.

**Fig. 7** Surface of polished SPS 1450 after etching at 1100 °C with the initial grains and the recrystallized grains which appear in scratches still left on the surface after polishing.

Figure 1  
[Click here to download high resolution image](#)

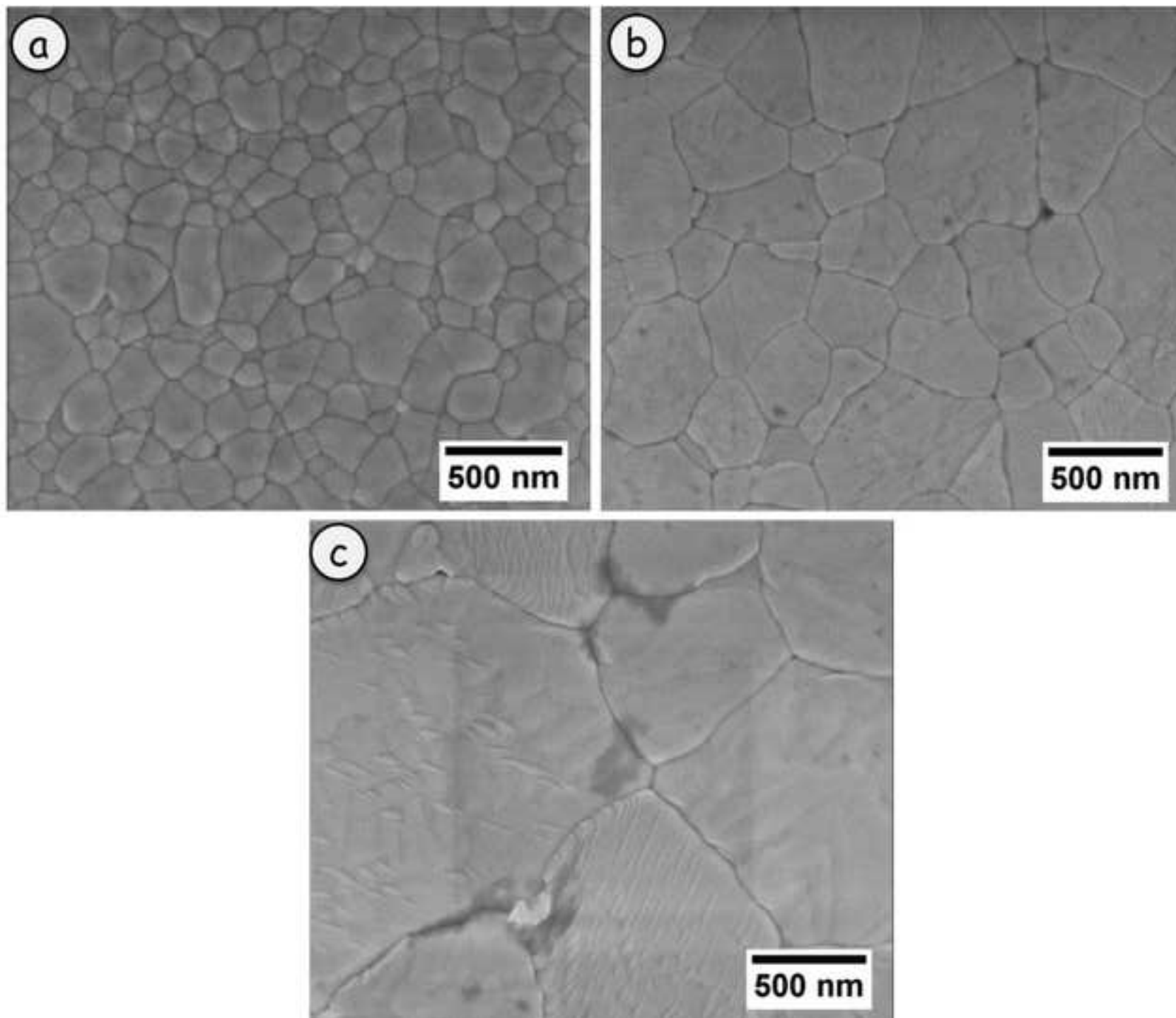


Figure 2  
[Click here to download high resolution image](#)

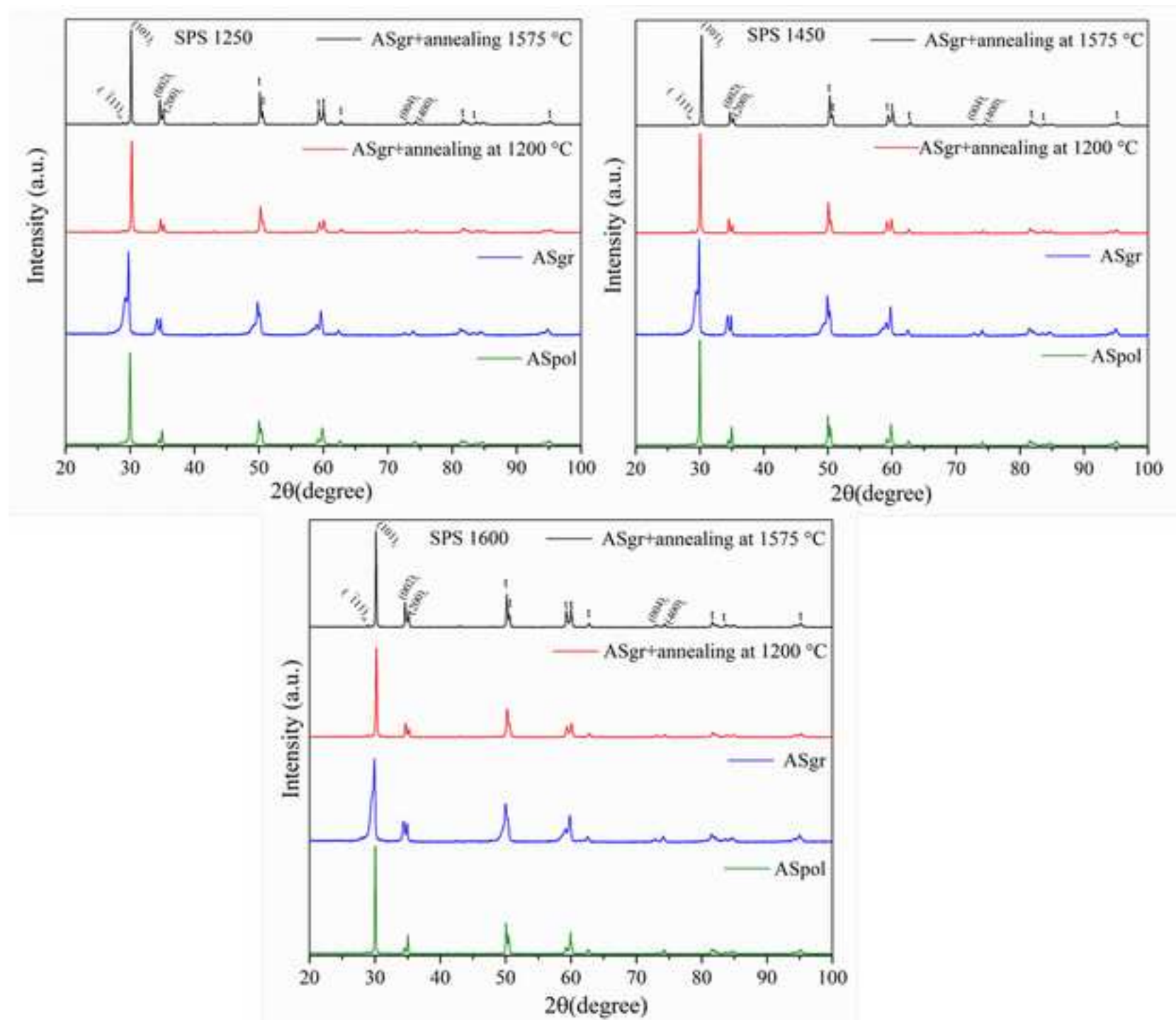


Figure 3  
[Click here to download high resolution image](#)

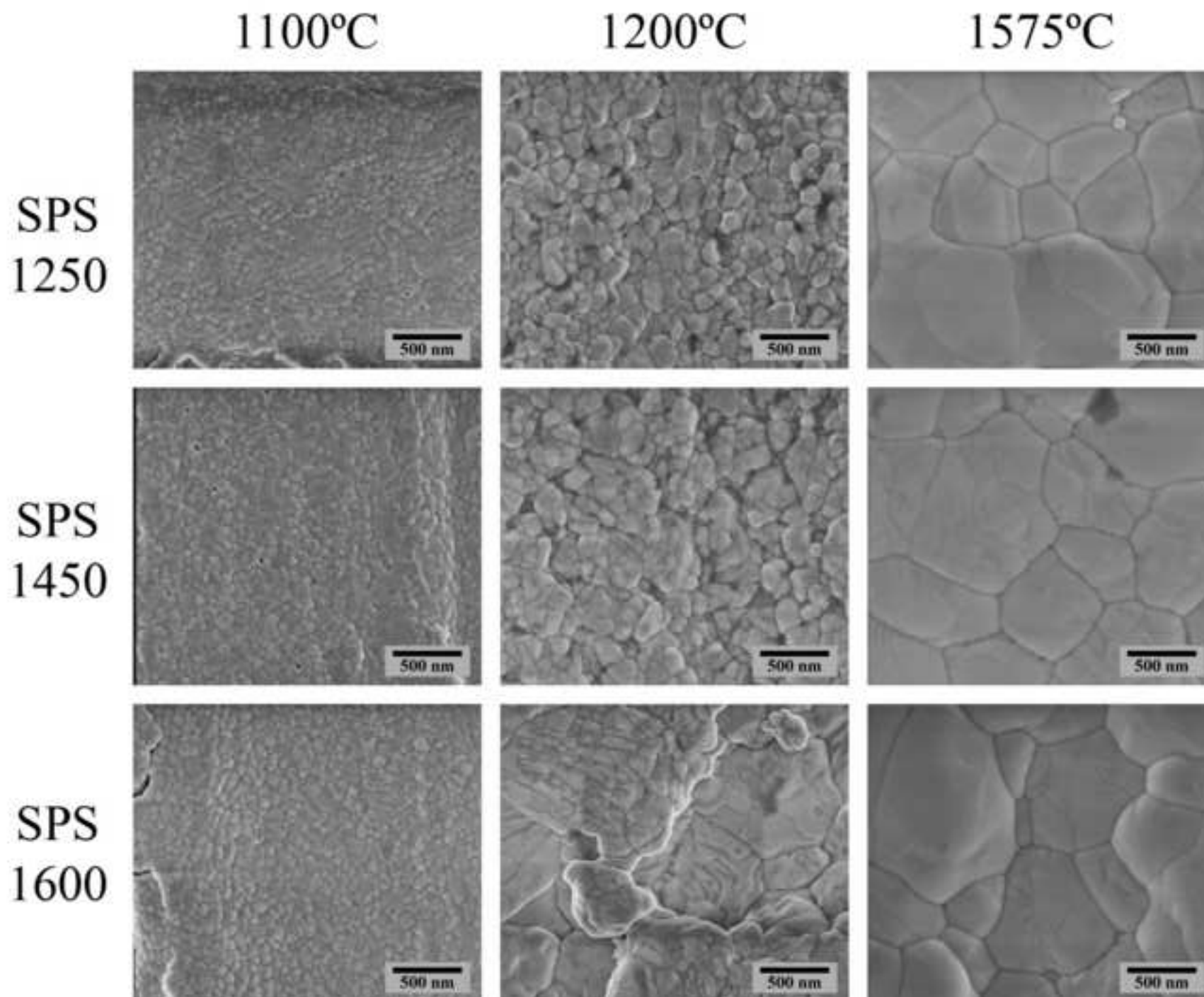


Figure 4  
[Click here to download high resolution image](#)

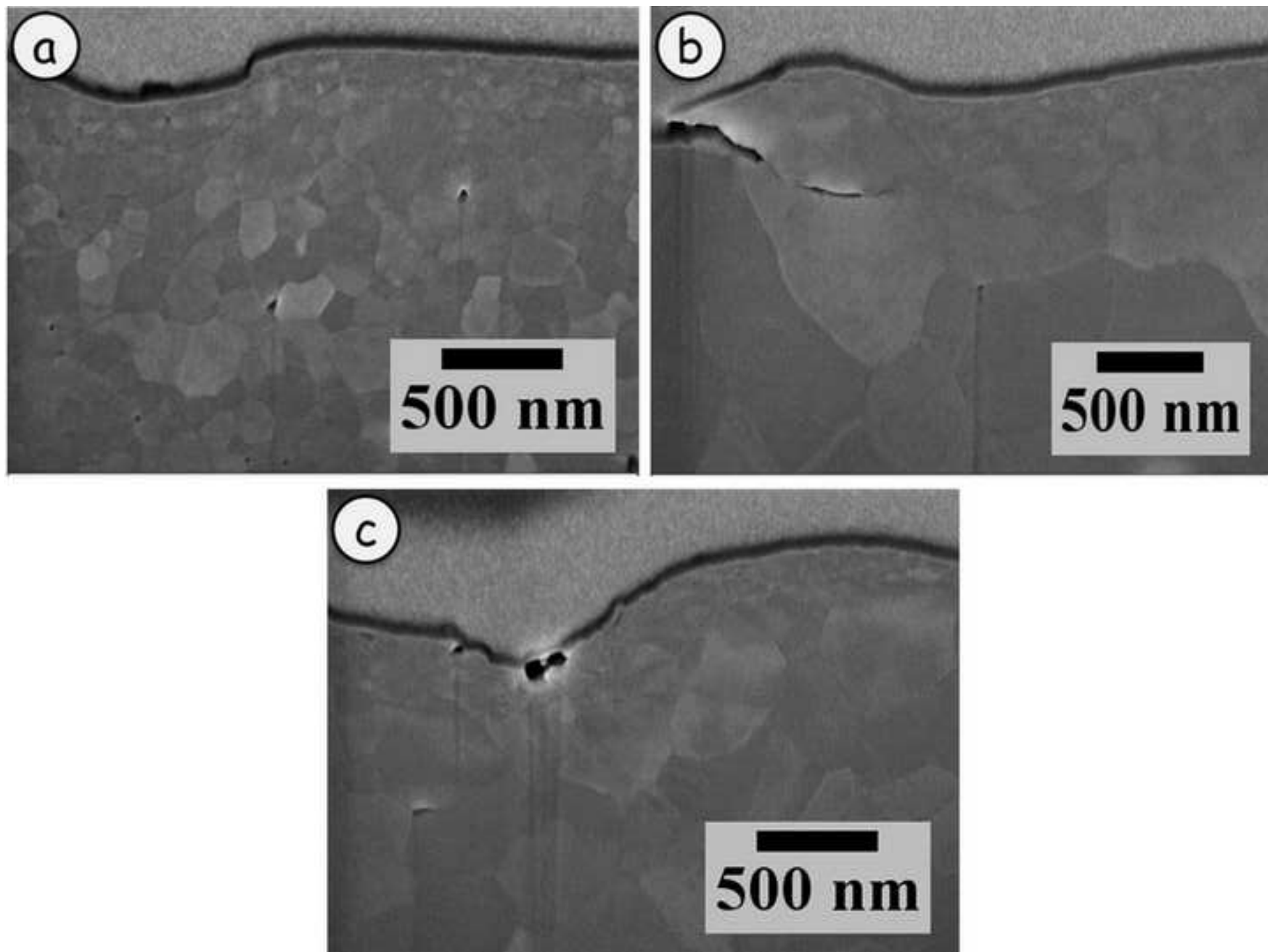


Figure 5  
[Click here to download high resolution image](#)

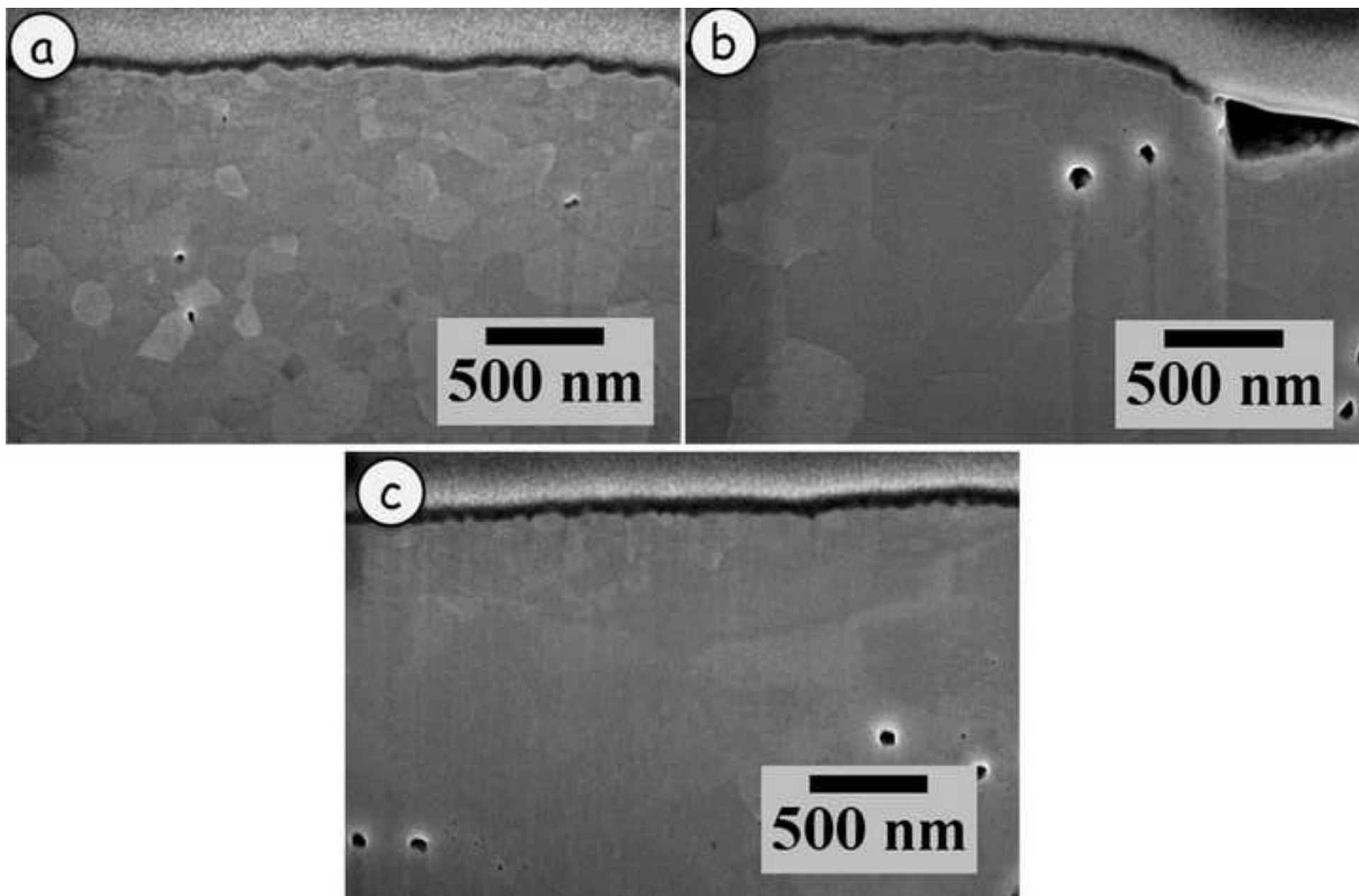




Figure 6  
[Click here to download high resolution image](#)

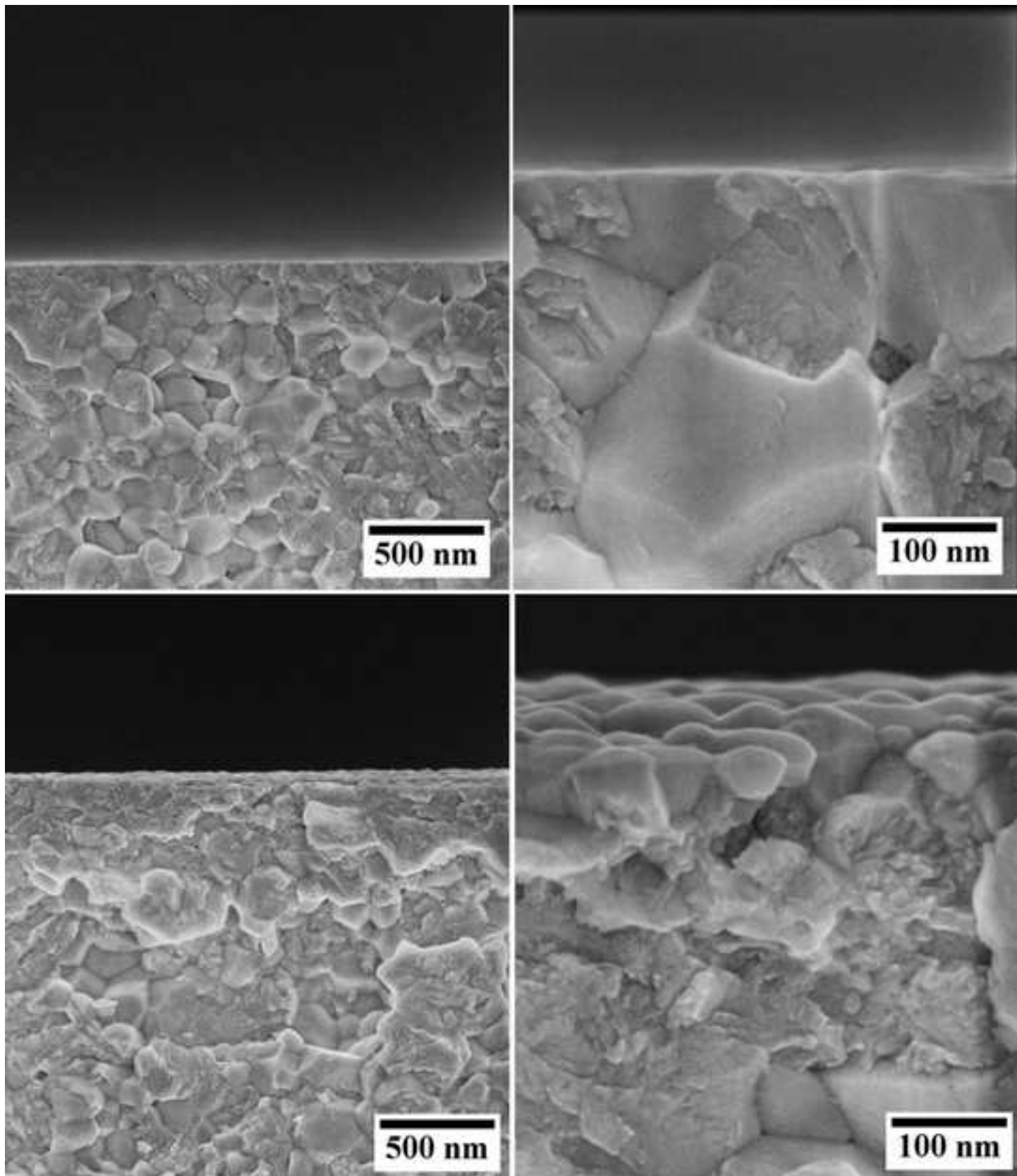


Figure 7  
[Click here to download high resolution image](#)

